

# Recovering Ground Truth Singular Values From Randomly Perturbed MIMO Transfer Functions

M.A. Bakhit<sup>1</sup>, F.A. Khattak<sup>1</sup>, G.W. Rice<sup>2</sup>, I.K. Proudler<sup>1</sup>, and S. Weiss<sup>1</sup>

<sup>1</sup>Department of Electronic and Electrical Engineering, University of Strathclyde, Glasgow, Scotland

<sup>2</sup>Mathworks Ltd., Glasgow, Scotland

**Abstract**—We show that analytic singular values of randomly perturbed matrices lose intersections and zero crossings compared to the unperturbed ground truth with probability one. As a result, the extracted singular values can significantly vary from the ground truth ones and may require a much high approximation order. To recover a solution closer to the ground truth, we extend a recent approach to extract ground truth analytic eigenvalues from a parahermitian matrix to the specific properties of analytic singular values. This method identifies segments where singular values are well separated, aligns them via partial reconstructions, and then performs an extraction based on the aligned segments. We demonstrate the approach in examples and ensemble simulations, thus highlighting its impact for applications that rely on solutions with low approximation order, and hence low implementation cost and latency.

## I. INTRODUCTION

In order to diagonalise a matrix of transfer functions  $A(z)$  that is analytic in  $z \in \mathbb{C}$ , one can use an analytic singular value decomposition (SVD) that has recently been proven to exist [1]–[3]. This allows to generalise the application of the SVD for standard matrices [4]–[6], such as for precoding and equalisation of narrowband channel matrices containing complex gain factors [7], to the case of broadband systems. Initial applications in the area [8]–[13] rely on polynomial SVD algorithms, which uses polynomials to approximate potentially piecewise analytic solutions. This leads to approximation orders that can be much higher than for the analytic SVD [2]. Thus, some algorithms have started to emerge for the latter [14], [15].

If  $A(z)$  has to be estimated, then estimation errors perturb the SVD factors [5]. Such a random perturbation has fundamental consequences for the analytic SVD factors, where the analytic singular values become strictly majorised and non-zero with probability one [16]. In this case, analytic and polynomial SVDs aim for the same solution, which likely requires a high approximation order with considerable impact on implementations [17]. A similar phenomenon is known from the analytic eigenvalue decomposition (EVD) when perturbed [18].

Therefore, in this paper we propose a method to recover the ground truth singular values based on a similar approach for analytic EVD in [19], but adapt this method to specifically recover zero crossings of ground truth singular values. Below, we review the analytic SVD, illustrate the loss of intersections

and zero-crossings for singular values on the unit circle, and propose modifications to the ‘eigenbone’ approach in [19]. We illustrate the operation of the proposed method in examples and ensemble simulations.

## II. ANALYTIC SVD

For almost all matrices  $A(z) : \mathbb{C} \rightarrow \mathbb{C}^{M \times N}$  that are analytic in  $z \in \mathbb{C}$ , there exists an analytic singular value decomposition

$$A(z) = U(z)\Sigma(z)V^P(z), \quad (1)$$

such that  $U(z) : \mathbb{C} \rightarrow \mathbb{C}^{M \times M}$  and  $V(z) : \mathbb{C} \rightarrow \mathbb{C}^{N \times N}$  are analytic paraunitary matrices, and  $\Sigma(z)$  is analytic, diagonal, and parahermitian [1], [2]. Paraunitarity implies that  $\{U(z)\}^{-1} = U^P(z) = \{U(1/z^*)\}^H$  with  $\{\cdot\}^P$  the parahermitian transposition [20], while a matrix being parahermitian means that  $\Sigma^P(z) = \Sigma(z)$  and thus  $\Sigma(e^{j\Omega}) \in \mathbb{R}$ .

For singular values to be analytic, they must be permitted to change sign. This may appear surprising, since this differs from the SVD of ordinary matrices where singular values are constrained to be non-negative real [6]. Lifting this constraint is also known to be required for the analytic singular value decomposition of matrices  $A(t)$  that are analytic on a real interval  $t$  [21], [22], and leads to a sign ambiguity of the singular values. The following example serves as an illustration.

*Example 1:* Consider the matrix

$$A(z) = \frac{1}{\sqrt{2}} \begin{bmatrix} e^{-j\frac{\pi}{4}} & e^{j\frac{\pi}{4}} \\ e^{j\frac{\pi}{4}} & e^{-j\frac{\pi}{4}} \end{bmatrix} + \mathbf{I}z^{-1} + \begin{bmatrix} e^{j\frac{\pi}{4}} & e^{-j\frac{\pi}{4}} \\ e^{-j\frac{\pi}{4}} & e^{j\frac{\pi}{4}} \end{bmatrix} \frac{z^{-2}}{\sqrt{2}}, \quad (2)$$

which admits an analytic SVD with  $U(z) = z^{-1}\mathbf{T}_2$  and  $V(z) = \mathbf{T}_2$ , where  $\mathbf{T}_N$  is an  $N$ -point DFT matrix normalised to be unitary. For  $\Sigma(z) = \text{diag}\{\sigma_1(z), \sigma_2(z)\}$ , the singular values are  $\sigma_1(z) = z + 1 + z^{-1}$  and  $\sigma_2(z) = 1 + \frac{1}{2}(jz^{-1} - jz)$ ; their evaluation on the unit circle is shown in Fig. 1. Either or both of these singular values could be negated, and the signs be absorbed into either the corresponding left- or right-singular vectors.  $\triangle$

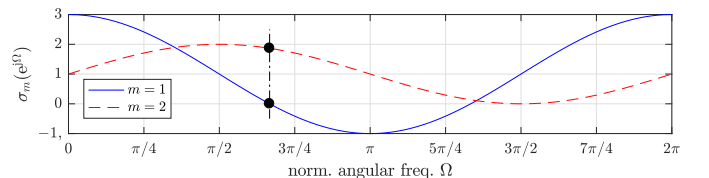


Fig. 1. Singular values of Example 1 evaluated on the unit circle. Markers indicate where for  $\Omega_0 = \frac{2}{3}\pi$  singular values are evaluated in Example 2.

M.A. Bakhit is funded by Mathworks Ltd and the University of Strathclyde. F.A. Khattak is the recipient of a scholarship of the Commonwealth Scholarship Commission.

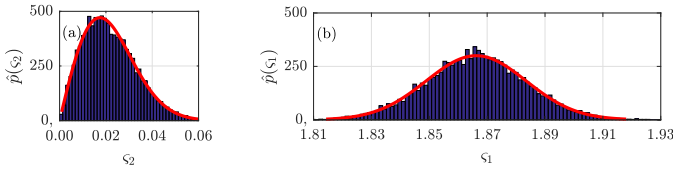


Fig. 2. Estimated distributions of  $\varsigma_m$ ,  $m = 1, 2$ , for the randomly perturbed matrix of Example 1 evaluated at  $\Omega_0 = \frac{2}{3}\pi$ , and Rician fits.

Current algorithms for the retrieval of the analytic SVD operate in the DFT domain, whereby first the analytic singular values have to be extracted by identifying the correct associations across bins; this then permits to associate the correct pairs of singular vectors across bins. A phase ambiguity to the singular vectors remains in each bin, and can be addressed by phase smoothing across bins akin to analytic EVD approaches [23], [24]. Crucial however is to first retrieve analytic singular values in order to establish associations across bins, and to subsequently extract singular vectors. Hence, we here focus on the challenge of extracting singular values.

### III. PERTURBATION OF SINGULAR VALUES

If an analytic matrix  $\mathbf{A}(z)$  is estimated e.g. via system identification [25], [26], then we measure a perturbed system

$$\hat{\mathbf{A}}(z) = \mathbf{A}(z) + \mathbf{E}(z), \quad (3)$$

where  $\mathbf{E}(z)$  represents the estimation error. We first assess the effect of this estimation error at a single frequency before considering the entire spectrum.

#### A. Bin-Wise Perturbation Perspective

If on the unit circle and for a particular normalised angular frequency  $\Omega_0$ ,  $\sigma_m$ ,  $m = 1, \dots, M$  are the singular values of  $\mathbf{A}(z)|_{z=e^{j\Omega_0}}$ , then for the SVD of  $\hat{\mathbf{A}}(z)|_{z=e^{j\Omega_0}}$  its singular values  $\varsigma_m$  have become stochastic quantities that obey some probability distributions. If at  $\Omega_0$ ,  $\mathbf{A}(e^{j\Omega_0})$  possesses a  $C$ -fold multiplicity of singular values, then because they are sampled from a distribution, the probability for repeated values of  $\varsigma_m$  is zero.

If ground truth singular values  $\sigma_m$  tend to zero, distributions of  $\varsigma$  are generally difficult to express, but for specific cases, examples are given in e.g. [27]–[29]. In general, the estimation error causes  $\varsigma_m$  to have a non-vanishing offset term [5], [16], i.e. we find that  $\varsigma_m \neq 0$  with probability one.

*Example 2:* Matrix  $\mathbf{A}(z)$  of Example 1 is perturbed in every element by complex Gaussian noise of variance  $10^{-2}$ . A total number of  $10^4$  such perturbations are generated, and the singular values  $\varsigma_m$ ,  $m = 1, 2$  are evaluated at  $\Omega_0 = \frac{2}{3}\pi$ , as indicated in Fig. 1. The ground truth singular values are  $\sigma_1(e^{j\Omega_0}) = 1 + \frac{1}{2}\sqrt{3}$  and  $\sigma_2(e^{j\Omega_0}) = 0$ . The estimated distributions of  $\varsigma_m$  are shown in Fig. 2, together with fitted Rician distributions.  $\triangle$

#### B. Perturbation Across the Spectrum

Let  $\hat{\sigma}_m(z)$  be the analytic singular values of  $\hat{\mathbf{A}}(z)$ . Sec. III-A has established that at a given frequency  $\Omega_0$ , the singular values  $\hat{\sigma}_m(e^{j\Omega_0}) = \varsigma_m$  with probability one will only

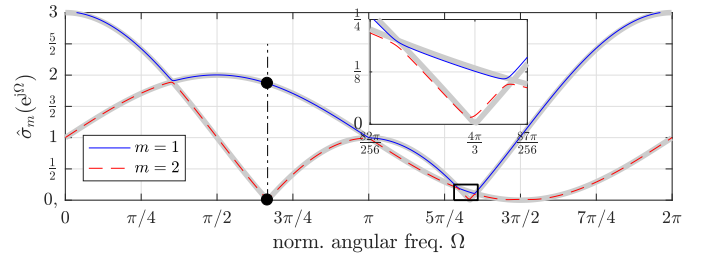


Fig. 3. Singular values  $\hat{\sigma}_m$ ,  $m = 1, 2$ , of Example 3 for the estimated matrix  $\hat{\mathbf{A}}(z)$ , evaluated on the unit circle; the ground truth is underlaid in grey.

have trivial multiplicities and not be zero. This of course holds at any given frequency; therefore with probability one, the singular values  $\hat{\sigma}_m(e^{j\Omega})$  across the entire spectrum will neither intersect each other — akin to eigenvalues of randomly perturbed parahermitian matrices [18] — nor the zero line.

*Example 3:* For a sufficiently fine evaluation of bin-wise SVDs along the unit circle, Fig. 3 shows the analytic singular values  $\hat{\sigma}_m(e^{j\Omega})$ ,  $m = 1, 2$ , of matrix  $\mathbf{A}(z)$  of Example 1 perturbed in every element by complex Gaussian noise of variance  $10^{-4}$ . With the ground truth illustrated in Fig. 1, the insert in Fig. 3 demonstrates how both intersections and zero crossings are lost due to the perturbation.  $\triangle$

As a consequence, it is difficult to recover the ground truth singular values from a randomly perturbed matrix. If the perturbation is reduced, e.g. through estimation based on a larger sample size  $N$  for the data, paradoxically the problem is only exaggerated: for large  $N$ , the singular values start to approach piecewise analytic functions, which require potentially very high approximation orders. The issue is only resolved for the transition  $N \rightarrow \infty$ .

### IV. PROPOSED ANALYTIC SINGULAR VALUE EXTRACTION

To recover the ground truth singular values from a randomly perturbed matrix  $\hat{\mathbf{A}}(z)$ , we adapt the approach for the analytic EVD in [19]. We modify this method to account for any sign changes in the ground truth singular values. The three component of the algorithm are addressed in turn.

#### A. Segmentation

Since DFT-domain approaches perform a bin-wise SVD with  $\hat{\mathbf{A}}(e^{j\Omega}) = \mathbf{U}_k \mathbf{\Sigma}_k \mathbf{V}_k^H$ ,  $k = 0, \dots, (K - 1)$  for DFT size of  $K$ , the challenge is to re-establish the association the values in the bins with the analytic functions [23], [24], [30]. This is a simple task where analytic singular values in  $\mathbf{\Sigma}_k$  are well-separated, but difficult where they are not. The key idea in [19] is to exploit the analyticity of the ground truth singular values, which theoretically allows us to reconstruct such functions entirely from any small segment within the region of convergence, including the unit circle. Therefore the aim is to find frequency bands where segments of analytic singular values can be identified.

For the segmentation, we assume singular values  $\mathbf{\Sigma}_k = \text{diag}\{\sigma_{1,k}, \dots, \sigma_{M,k}\}$  with  $\sigma_{1,k} \geq \sigma_{2,k} \geq \dots \geq \sigma_{M,k}$  and determine the smallest difference  $\delta_k = \min_{m \in \{1, \dots, M\}} (\sigma_{m,k} - \sigma_{m+1,k})$ . We define an extra element  $\sigma_{M+1,k} := -\sigma_{M,k}$ , such

## Recovering ground truth singular values from randomly perturbed MIMO transfer functions

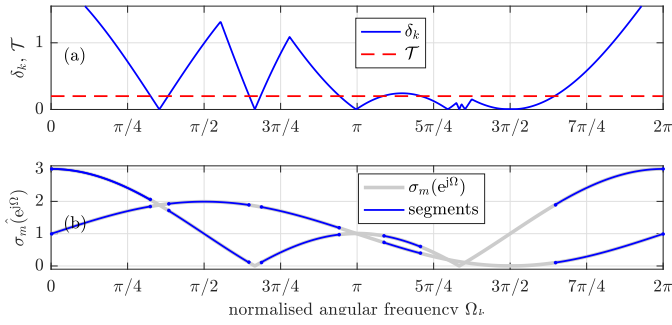


Fig. 4. (a) Minimum singular value distance  $\delta_k$  and threshold  $\mathcal{T}$ , and (b)  $Q = 4$  analytic segments of singular values of  $\mathbf{A}(z)$  from Example 3.

that  $\delta_k$  represents the smallest difference between any singular values, including negative ones. A segment is then identified as an interval of consecutive frequency bins between upper and lower frequencies  $\Omega_u$  and  $\Omega_l$ , such that

$$\max_{\Omega_u, \Omega_l} (\Omega_u - \Omega_l) \quad \text{s.t.} \quad \delta_k > \mathcal{T}, \quad \forall \Omega_k \in [\Omega_l, \Omega_u], \quad (4)$$

where  $\mathcal{T}$  is a predefined threshold for the minimum separation of singular values. For a meaningful segmentation, we only retain segments that stretch over a minimum number  $L$  of frequency bins, such that further  $(\Omega_u - \Omega_l) > \frac{2\pi L}{K}$  is fulfilled.

*Example 4:* To demonstrate the segmentation process, we utilise  $\mathbf{A}(z)$  from Example 3 with singular values in Fig. 3 and their ground truth in Fig. 1. Fig. 4(a) shows the distance  $\delta_k$  per bin for a  $K = 1024$ -point DFT. With a threshold  $\mathcal{T} = \frac{1}{10} \max_k \delta_k$  and  $L = 16$ ,  $Q = 4$  segments arise as shown in Fig. 4(b), with the first segment wrapped at  $\Omega = 0$ .  $\triangle$

### B. Alignment

To align or associate the segments identified in Sec. IV-A, we will compare partial reconstructions of  $Q$  different segments with each other. For the partial reconstruction  $s_{q,m}[\tau]$  of the  $m$ th singular value in the  $q$ th segment containing bin frequencies in the set  $\mathcal{W}_q$ , a partial IDFT can be formulated as the least squares problem

$$s_{q,m}[\tau] = \arg \min_{s[\tau]} \sum_{\Omega_k \in \mathcal{W}_q} \left| \sum_{\tau=-T}^T s[\tau] e^{-j\Omega_k \tau} - \sigma_{m,k} \right|^2. \quad (5)$$

This reconstruction is evaluated over a support  $|\tau| \leq T$ ; for small  $T$ , this emphasises the smooth or lowpass nature of the reconstruction.

*Example 5:* Partial reconstructions of the segments from Fig. 4 according to (5) with  $T = 2$  are shown in Fig. 5. Each column  $q = 1, \dots, Q$  represents the reconstruction of one of the  $Q = 4$  segments. Note that the partial reconstructions  $s_{q,m}[\tau]$  closely match the ground truth singular values  $\sigma_i(z)$ ,  $i = 1, 2$ , from Example 1. It is therefore possible to visually determine which segments belong to which  $\sigma_m(e^{j\Omega})$ , as colour-coded by blue and red frames of the subplots. For the singular values marked in blue, the reconstructions in segments  $q = 2$  and  $q = 3$  are negated w.r.t. the other segments, and indicate that a sign change should be applied in order to recover a singular value with zero crossings.  $\triangle$

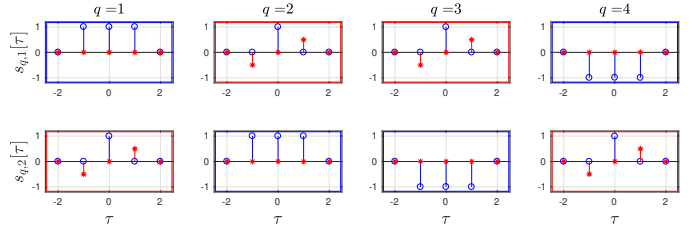


Fig. 5. Partial reconstructions  $s_{q,m}[\tau]$  of Example 5 with colour-coded frames to highlight associations across the  $Q = 4$  segments; real parts are marked in blue circles ( $\circ$ ), imaginary parts in red asterisks ( $*$ ).

The alignment can be established via [31], [32]. For simplicity, we utilise a covariance matrix  $\mathbf{C}_q$  for the alignment between the  $q$ th and the  $(q+1)$ th segment. For the element  $c_{q,m,\mu}$  in the  $m$ th row and  $\mu$ th column of  $\mathbf{C}_q$ , we calculate

$$c_{q,m,\mu} = \frac{\sum_{\tau} s_{q,m}[\tau] s_{q+1,\mu}^*[\tau]}{\sqrt{(\sum_{\tau} |s_{q,m}[\tau]|^2)(\sum_{\tau} |s_{q+1,\mu}[\tau]|^2)}}. \quad (6)$$

The row- or column-wise maxima of  $|c_{q,m,n}|$  indicate the permutation, while the sign of the modulus-maximum covariance coefficient indicates whether a sign change is required.

### C. Singular Value Retrieval

If  $\tilde{s}_{q,m}[\tau]$  represents the aligned and sign-corrected partial reconstructions from Sec. IV-B, then we now reconstruct the estimated ground truth singular values. Since longer segments are more reliable, we perform this as a segment-sized average

$$\hat{\sigma}_m[\tau] = \sum_{q=1}^Q \frac{|\mathcal{W}_q|}{|\mathcal{W}_1 \cup \dots \cup \mathcal{W}_Q|} \tilde{s}_{q,m}[\tau], \quad (7)$$

where  $|\cdot|$  denotes the cardinality of a set. When comparing the retrieved singular values  $\hat{\sigma}_m(z)$  to the ground truth analytic singular values  $\sigma_m(z)$ , note that they may differ in ordering and sign in accordance with the ambiguities of the analytic SVD in Sec. II.

## V. SIMULATIONS AND RESULTS

### A. Simulation Scenario

We assume a randomised matrix  $\mathbf{A}(z)$  of dimension  $M = 3$  of temporal support  $N$ , that is constructed from its known analytic SVD factors in (1). While  $\mathbf{U}(z)$  and  $\mathbf{V}(z)$  can be constructed from a sequence of random elementary paraunitary matrices [20], for the singular values, we assume a polynomial  $s_m(z)$  with zero mean complex Gaussian coefficients, and create a singular value via  $\sigma'_m(z) = s_m(z) + s_m^P(z)$ . The matrix of singular values  $\mathbf{\Sigma}(z) = \gamma \text{diag}\{\sigma'_1(z), \sigma'_2(z), \sigma'_3(z)\}$ , where  $\gamma$  is a normalisation factor.

A noisy  $\hat{\mathbf{A}}(z)$  according to (3) is created by a perturbation term  $\mathbf{E}(z)$  with independent complex Gaussian coefficients of variance  $\sigma_e^2$ , and the same temporal support as  $\mathbf{A}(z)$ . To assess the level of perturbation, we define a ‘system to noise’ ratio (SNR)  $\rho$  based on the energy  $\xi_{\mathbf{A}(z)}$  in a polynomial matrix  $\mathbf{A}(z)$ , defined as

$$\xi_{\mathbf{A}(z)} = \sum_n \|\mathbf{A}[n]\|_F^2. \quad (8)$$

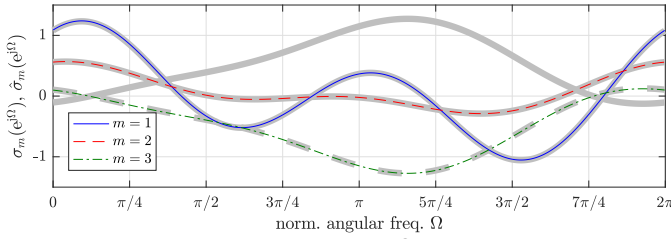


Fig. 6. Ground truth singular values  $\sigma_m(e^{j\Omega})$  overlaid in solid grey, and retrieved singular values  $\hat{\sigma}_m(e^{j\Omega})$  in colour;  $\hat{\sigma}_3(e^{j\Omega})$  is negated, and matches  $-\sigma_3(e^{j\Omega})$  (underlaid in dashed grey).

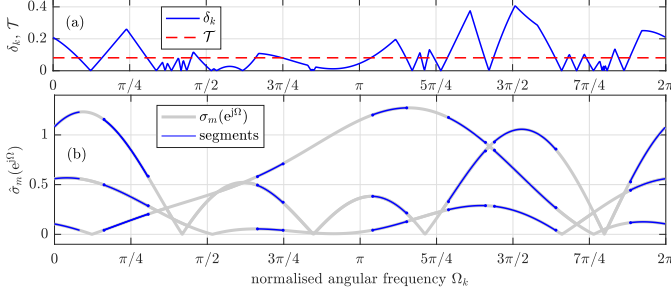


Fig. 7. (a) Minimum distance  $\delta_k$  and (b) the identified  $Q = 6$  segments.

Note that due to Parseval's theorem [33] and the analytic SVD, for  $\xi_{\mathbf{A}(z)}$  we have that

$$\xi_{\mathbf{A}(z)} = \frac{1}{2\pi} \int_0^{2\pi} \|\mathbf{U}(e^{j\Omega})\Sigma(e^{j\Omega})\mathbf{V}^P(e^{j\Omega})\|_{\mathbb{F}}^2 d\Omega \quad (9)$$

$$= \frac{1}{2\pi} \int_0^{2\pi} \|\Sigma(e^{j\Omega})\|_{\mathbb{F}}^2 d\Omega = \sum_m \|\Sigma[m]\|_{\mathbb{F}}^2 = \xi_{\Sigma(z)}. \quad (10)$$

With  $\mathbf{E}(z)$  of temporal support  $N$ , we find that the SNR is  $\rho = \xi_{\mathbf{A}(z)}/\xi_{\mathbf{E}(z)} = \xi_{\Sigma(z)}/\xi_{\mathbf{E}(z)}$ . If the normalisation  $\gamma$  above is selected such that  $\xi_{\Sigma(z)} = 1$ , then the expected SNR will be  $\mathcal{E}\{\rho\} = (M^2 N \sigma_e^2)^{-1}$ .

### B. Worked Example

We first demonstrate the proposed method on a single instance of  $\hat{\mathbf{A}}(z)$ ; this is a slightly higher dimensional and more complicated system than in previous examples. Both  $\Sigma(z)$ , with its ground truth singular values shown in Fig. 6, and  $\mathbf{E}(z)$  have a temporal support of  $N = 5$ , and with  $\sigma_e^2 = 10^{-7}$ , the SNR  $\rho$  of  $\hat{\mathbf{A}}(z)$  is 53 dB. The algorithm operates with a DFT length of  $K = 2^{10}$ , a threshold  $\mathcal{T} = \frac{1}{5} \max_k \delta_k$ , and a minimum segment length of  $L = 16$ .

The minimum distance  $\delta_k$  of singular values and the threshold  $\mathcal{T}$  are shown in Fig. 7(a), resulting in the segmentation in Fig. 7(b) — which also shows the perturbed, non-negative analytic singular values of  $\hat{\mathbf{A}}(z)$  — with  $Q = 6$  segments. Their partial reconstructions are illustrated in Fig. 8, where the associations across segments are indicated in coloured subplot frames; with the first segment ( $q = 1$ ) being the frequency-wrapped segment from Fig. 7(b). The retrieved, segment-size weighted reconstruction of the singular values is overlaid in Fig. 6, and closely matches the ground truth; due to  $\sigma_3(e^{j\Omega})$  being negative in the first segment, due to the sign ambiguity of the singular values we retrieve  $\hat{\sigma}_3(z) \approx -\sigma_3(z)$ .

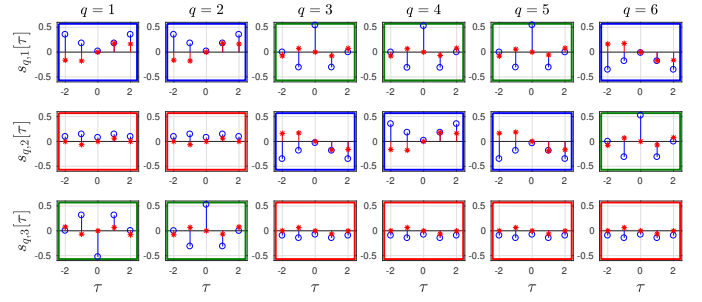


Fig. 8. Partial reconstructions  $s_{q,m}[\tau]$  of segments, with the frame colours encoding the alignment; real parts of  $s_{q,m}[\tau]$  are marked in blue circles (o), imaginary parts in red asterisks (\*).

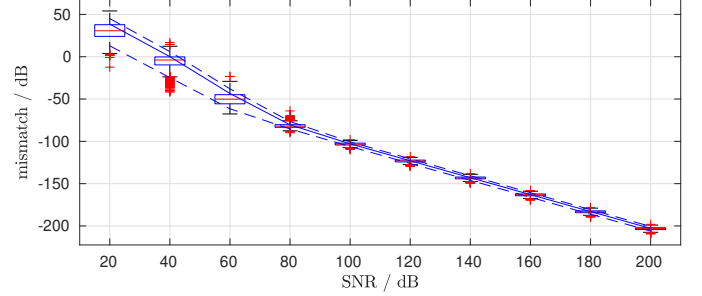


Fig. 9. Box plot with ensemble results for mismatch  $\xi_{\Sigma(z)-\hat{\Sigma}(z)}$  vs the SNR of the perturbation; the solid line indicates the mean, dashed lines the bounds within which 90% of the ensemble results reside.

### C. Ensemble Simulation

To demonstrate the proposed singular value retrieval over a larger set of simulations, we present results over an ensemble of  $10^3$  randomisations of both  $\mathbf{A}(z)$  and  $\mathbf{E}(z)$  for  $M = 3$  and  $N = 5$ , and for various SNRs ranging from 20 dB to 200 dB. The system of Sec. V-B is one instantiation of this ensemble. In order to assess the performance, we compare the difference between the unperturbed ground truth singular values in  $\Sigma(z)$  with the (potentially re-ordered and sign-corrected) retrieved values in  $\hat{\Sigma}(z)$ . To assess this difference, we use the least squares mismatch  $\xi_{\Sigma(z)-\hat{\Sigma}(z)}$ .

The results in Fig. 9 indicates that at higher SNRs above 70 dB, the proposed method very accurately retrieves the ground truth with an error equivalent to the perturbation. At lower SNRs, the performance degrades at a level higher than the perturbation power but still gradually. At low SNR, the perturbation will be such that identified segments do not necessarily provide an accurate enough partial reconstruction to permit alignment across the spectrum.

## VI. CONCLUSIONS

We have shown that random perturbations to a matrix of transfer functions cause its analytic singular values to lose any intersections and zero-crossings. To retrieve smooth singular values with short support — and hence implementations with low cost and potentially latency — we have proposed a method to retrieve singular values close to the ground truth. Illustrations and an ensemble simulation for modestly-dimensional matrices indicate that this is a promising route to retrieve solutions close to the ground truth.

## REFERENCES

- [1] G. Barbarino and V. Noferini, "On the Rellich eigendecomposition of para-Hermitian matrices and the sign characteristics of  $*$ -palindromic matrix polynomials," *Linear Algebra and its Applications*, vol. 672, pp. 1–27, Sep. 2023.
- [2] S. Weiss, I. K. Proudler, G. Barbarino, J. Pestana, and J. G. McWhirter, "On properties and structure of the analytic singular value decomposition," *IEEE Transactions on Signal Processing*, vol. 72, pp. 2260–2275, 2024.
- [3] G. Barbarino, "On the periodicity of singular vectors and the holomorphic block-circulant SVD on the unit circumference," *Linear Algebra and its Applications*, Dec 2024.
- [4] G. Strang, *Linear Algebra and Its Applications*, 2nd ed. New York: Academic Press, 1980.
- [5] G. W. Stewart and J.-g. Sun, *Matrix Perturbation Theory*. Academic Press, 1990.
- [6] G. H. Golub and C. F. Van Loan, *Matrix Computations*, 3rd ed. Baltimore, Maryland: John Hopkins University Press, 1996.
- [7] M. Vu and A. Paulraj, "MIMO Wireless Linear Precoding," *IEEE Signal Processing Magazine*, vol. 24, no. 5, pp. 86–105, Sep. 2007.
- [8] J. G. McWhirter, P. D. Baxter, T. Cooper, S. Redif, and J. Foster, "An EVD Algorithm for Para-Hermitian Polynomial Matrices," *IEEE Transactions on Signal Processing*, vol. 55, no. 5, pp. 2158–2169, May 2007.
- [9] C. H. Ta and S. Weiss, "A Jointly Optimal Precoder and Block Decision Feedback Equaliser Design With Low Redundancy," in *15th European Signal Processing Conference*, Poznan, Poland, September 2007, pp. 489–492.
- [10] W. Al-Hanafy, A. P. Millar, C. H. Ta, and S. Weiss, "Broadband SVD and non-linear precoding applied to broadband MIMO channels," in *42nd Asilomar Conference on Signals, Systems and Computers*, Pacific Grove, CA, USA, Oct. 2008, pp. 2053–2057.
- [11] H. Zamiri-Jafarian and M. Rajabzadeh, "A polynomial matrix svd approach for time domain broadband beamforming in MIMO-OFDM systems," in *VTC Spring 2008 - IEEE Vehicular Technology Conference*, 2008, pp. 802–806.
- [12] J. Foster, J. McWhirter, M. Davies, and J. Chambers, "An algorithm for calculating the qr and singular value decompositions of polynomial matrices," *IEEE Transactions on Signal Processing*, vol. 58, no. 3, pp. 1263–1274, March 2010.
- [13] N. Moret, A. Tonello, and S. Weiss, "MIMO precoding for filter bank modulation systems based on PSVD," in *IEEE 73rd Vehicular Technology Conference*, May 2011, pp. 1–5, (best paper award).
- [14] M. A. Bakhit, F. A. Khattak, I. K. Proudler, S. Weiss, and G. W. Rice, "Compact order polynomial singular value decomposition of a matrix of analytic functions," in *9th IEEE international Workshop on Computational Advances in Multi-Sensor Adaptive Processing*, Los Sueños, Costa Rica, Dec. 2023.
- [15] F. A. Khattak, M. Bakhit, I. K. Proudler, and S. Weiss, "Extraction of analytic singular values of a polynomial matrix," in *32nd European Signal Processing Conference*, Lyon, France, August 2024, pp. 1297–1301.
- [16] M. Bakhit, F. A. Khattak, I. K. Proudler, and S. Weiss, "Impact of estimation errors of a matrix of transfer functions onto its analytic singular values and their potential algorithmic extraction," in *IEEE High Performance Extreme Computing Conference*. Boston, MA: IEEE, Sep. 2024, pp. 1–7.
- [17] F. K. Coutts, I. K. Proudler, and S. Weiss, "Efficient implementation of iterative polynomial matrix evd algorithms exploiting structural redundancy and parallelisation," *IEEE Transactions on Circuits and Systems I: Regular Papers*, vol. 66, no. 12, pp. 4753–4766, Dec. 2019.
- [18] F. A. Khattak, S. Weiss, I. K. Proudler, and J. G. McWhirter, "Space-time covariance matrix estimation: Loss of algebraic multiplicities of eigenvalues," in *56th Asilomar Conference on Signals, Systems, and Computers*, Pacific Grove, CA, Oct. 2022.
- [19] S. J. Schlecht and S. Weiss, "Reconstructing analytic dinosaurs: Polynomial eigenvalue decomposition for eigenvalues with unmajorised ground truth," in *32nd European Signal Processing Conference*, Lyon, France, August 2024, pp. 1287–1291.
- [20] P. P. Vaidyanathan, *Multirate Systems and Filter Banks*. Englewood Cliffs: Prentice Hall, 1993.
- [21] B. De Moor and S. Boyd, "Analytic properties of singular values and vectors," KU Leuven, Tech. Rep., 1989.
- [22] A. Bunse-Gerstner, R. Byers, V. Mehrmann, and N. K. Nicols, "Numerical computation of an analytic singular value decomposition of a matrix valued function," *Numer. Math.*, vol. 60, pp. 1–40, 1991.
- [23] S. Weiss, I. K. Proudler, and F. K. Coutts, "Eigenvalue decomposition of a parahermitian matrix: extraction of analytic eigenvalues," *IEEE Transactions on Signal Processing*, vol. 69, pp. 722–737, 2021.
- [24] S. Weiss, I. Proudler, F. Coutts, and F. Khattak, "Eigenvalue decomposition of a parahermitian matrix: extraction of analytic eigenvectors," *IEEE Transactions on Signal Processing*, vol. 71, pp. 1642–1656, Apr. 2023.
- [25] B. Widrow and S. D. Stearns, *Adaptive Signal Processing*. Englewood Cliffs, New York: Prentice Hall, 1985.
- [26] S. Haykin, *Adaptive Filter Theory*, 2nd ed. Englewood Cliffs: Prentice Hall, 1991.
- [27] J.-M. Azaïs and M. Wschebor, "Upper and lower bounds for the tails of the distribution of the condition number of a Gaussian matrix," *SIAM Journal on Matrix Analysis and Applications*, vol. 26, no. 2, pp. 426–440, 2004.
- [28] T. Ratnarajah, R. Vaillancourt, and M. Alvo, "Eigenvalues and condition numbers of complex random matrices," *SIAM Journal on Matrix Analysis and Applications*, vol. 26, no. 2, pp. 441–456, 2004.
- [29] W. Anderson and M. T. Wells, "The exact distribution of the condition number of a gaussian matrix," *SIAM Journal on Matrix Analysis and Applications*, vol. 31, no. 3, pp. 1125–1130, 2010.
- [30] M. Tohidian, H. Amindavar, and A. M. Reza, "A DFT-based approximate eigenvalue and singular value decomposition of polynomial matrices," *EURASIP Journal on Advances in Signal Processing*, vol. 2013, no. 1, pp. 1–16, 2013.
- [31] H. W. Kuhn, "The Hungarian method for the assignment problem," *Naval Research Logistics Quarterly*, vol. 2, no. 1-2, pp. 83–97, 1955.
- [32] D. Pachauri, R. Kondor, and V. Singh, "Solving the multi-way matching problem by permutation synchronization," in *Advances in Neural Information Processing Systems*, vol. 26, 2013.
- [33] B. Girod, R. Rabenstein, and A. Stenger, *Signals and Systems*. Chichester: J. Wiley & Sons, 2001.